

Salvianolic acid B inhibits growth of head and neck squamous cell carcinoma *in vitro* and *in vivo* via cyclooxygenase-2 and apoptotic pathways

Yubin Hao¹, Tianpei Xie², Alexandru Korotcov^{3,4}, Yanfei Zhou¹, Xiaowu Pang¹, Liang Shan^{3,4}, Hongguang Ji², Rajagopalan Sridhar^{3,5}, Paul Wang^{3,4}, Joseph Califano⁶ and Xinbin Gu^{1,3*}

¹Department of Oral Diagnostic Service, Howard University, Washington, DC

²Shanghai TenGen Biomedical Co. Ltd, Shanghai

³Department of Cancer Center, Howard University, Washington, DC

⁴Department of Radiology, Howard University, Washington, DC

⁵Department of Radiation Oncology, Howard University, Washington, DC

⁶Department of Otolaryngology-Head and Neck Surgery, Johns Hopkins University, Baltimore, MD

Overexpression of cyclooxygenase-2 (COX-2) in oral mucosa has been associated with increased risk of head and neck squamous cell carcinoma (HNSCC). Celecoxib is a nonsteroidal anti-inflammatory drug, which inhibits COX-2 but not COX-1. This selective COX-2 inhibitor holds promise as a cancer preventive agent. Concerns about cardiotoxicity of celecoxib, limits its use in long-term chemoprevention and therapy. Salvianolic acid B (Sal-B) is a leading bioactive component of *Salvia miltiorrhiza* Bge, which is used for treating neoplastic and chronic inflammatory diseases in China. The purpose of this study was to investigate the mechanisms by which Sal-B inhibits HNSCC growth. Sal-B was isolated from *S. miltiorrhiza* Bge by solvent extraction followed by 2 chromatographic steps. Pharmacological activity of Sal-B was assessed in HNSCC and other cell lines by estimating COX-2 expression, cell viability and caspase-dependent apoptosis. Sal-B inhibited growth of HNSCC JHU-022 and JHU-013 cells with IC₅₀ of 18 and 50 μM, respectively. Nude mice with HNSCC solid tumor xenografts were treated with Sal-B (80 mg/kg/day) or celecoxib (5 mg/kg/day) for 25 days to investigate *in vivo* effects of the COX-2 inhibitors. Tumor volumes in Sal-B treated group were significantly lower than those in celecoxib treated or untreated control groups ($p < 0.05$). Sal-B inhibited COX-2 expression in cultured HNSCC cells and in HNSCC cells isolated from tumor xenografts. Sal-B also caused dose-dependent inhibition of prostaglandin E₂ synthesis, either with or without lipopolysaccharide stimulation. Taken together, Sal-B shows promise as a COX-2 targeted anticancer agent for HNSCC prevention and treatment.

© 2008 Wiley-Liss, Inc.

Key words: salvianolic acid B; head and neck cancer; cancer therapy; COX-2; apoptosis

Head and neck squamous cell carcinoma (HNSCC) is a major threat to global public health, with over 500,000 new cases annually worldwide.¹ In the United States, oral and pharyngeal cancers alone account for ~35,000 new cases.² While overall survival rates of head and neck cancers have improved modestly in recent years, African-American males are affected by HNSCC at younger ages of incidence, with increased mortality, and present with more advanced disease.^{2–5} HNSCC is thought to develop through a multistep, multifocal process that can involve field carcinogenesis and intraepithelial clonal spread.³ A normal epithelial cell can take many years to undergo the multiple cellular and genetic alterations that lead to malignant changes. Thus, it remains an appealing strategy to develop effective, nontoxic and affordable novel pharmacological agents for preventing development of HNSCC and second primary HNSCC.^{3,6–8}

Overexpression of cyclooxygenase-2 (COX-2) in the oral mucosa has been associated with increased risk of head and neck cancer.^{6,9–13} Several processes linked to carcinogenesis can be influenced by the enhanced synthesis of prostaglandin E₂ (PGE₂).^{14–17} Therefore, COX-2 has been intensively studied for development of chemopreventive agents. Celecoxib is a nonsteroidal anti-inflammatory drug (NSAID) that helps to control inflammation by inhibiting COX-2 activity without appreciable effect on COX-1 enzyme activity. In the last decade, numerous studies reported that

celecoxib reduces the risk for a variety of human cancers, including HNSCC in experimental systems, *via* COX-2-dependent and COX-2-independent pathways.^{7,18–21} Celecoxib is more potent and less toxic than traditional NSAIDs in inhibiting COX-2. However, celecoxib has been shown to cause adverse cardiovascular effects when taken at high doses over a long duration.²² Hence, it is important to develop effective, safer and selective COX-2 inhibitors for cancer prevention and treatment.

Salvia miltiorrhiza Bge (Danshen or Tanshen) is a well-known Chinese herbal medicine that has been used to reduce inflammatory reactions in cardiovascular, hepatic and tumoral diseases without appreciable adverse effects.^{23–26} *S. miltiorrhiza* Bge was first described in the Chinese pharmacology book *Shen Nong's Canon on Materia Medica* (circa 100–180 A.D.) and the medicinal properties of this plant have been extensively studied.^{24–26} Salvianolic acid B (Sal-B) is a depside, which is considered to be the active component of *S. miltiorrhiza* Bge. Thus, Sal-B is used as a quality control ingredient and active marker of *S. miltiorrhiza* Bge products by the National Pharmacopoeia Council of China.^{27,28} Importantly, recent studies have demonstrated the potential of Sal-B to inhibit tumor cell growth,^{25,29–31} inflammation^{25,32} and oxidation.^{33,34} We had demonstrated that Sal-B decreased cell proliferation and viability in 15 different cancer cell lines, including Hep G2 human liver cancer cells and AGS human stomach cancer cells.²⁸ In addition, Lin and coworkers³⁵ recently reported that Sal-B attenuates COX-2 expression in lipopolysaccharide (LPS)-treated human aortic smooth muscle cells. Taken together, these observations suggest that Sal-B is a promising anticancer agent for targeting COX-2 and cell growth for prevention and treatment of cancer. The ability of Sal-B to inhibit growth of HNSCC *in vitro* and *in vivo* was studied. The related mechanisms of action of Sal-B were investigated with respect to cell cycle progression, cell viability, apoptosis and gene expression.

Material and methods

Chemical reagents

5-Fluorouracil (5-FU), propidium iodide and lipopolysaccharide (LPS) were obtained from Sigma Chemical Company (St. Louis,

Abbreviations: COX-2, cyclooxygenase-2; FITC, fluorescein isothiocyanate; 5-FU, fluorouracil; HNSCC, head and neck squamous cell carcinoma; HPLC, high pressure liquid chromatography; LPS, lipopolysaccharide; MTT, 3-(4,5-Dimethylthiazol-2-yl)-2,5-diphenyltetrazolium bromide; MRI, magnetic resonance imaging; NF-κB, nuclear factor-kappa B; PARP, poly(ADP-ribose) polymerase; PBS, phosphate buffered saline; PGE₂, prostaglandin E₂; Sal-B, salvianolic acid B.

Grant sponsors: National Cancer Institute/NIH CA118770 and 5U54CA091431, and Tianjue Gu Foundation.

*Correspondence to: Department of Oral Diagnostic Service, Howard University College of Dentistry, 600 W Street, NW, Washington, DC 20059, USA. Fax: (202) 806-0447. E-mail: xgu@howard.edu

Received 29 August 2008; Accepted after revision 7 November 2008

DOI 10.1002/ijc.24160

Published online 19 November 2008 in Wiley InterScience (www.interscience.wiley.com).

MO). D101 Macroporous resin was obtained from Yiadong Chemical Company (Shanghai, China) and polyamide was obtained from Sinopharm Chemical Reagent Company (Shanghai, China). Celecoxib was extracted from commercially available 200 mg celebrexTM capsules with ethyl acetate in the presence of water. The organic extract was washed once with water and then dried with anhydrous sodium sulfate and then filtered. The organic solvent was removed using a rotary evaporator to obtain pure crystals of celecoxib.

Cell lines and culture

HNSCC cell lines (JHU-06, -011, -013, -019, -022 and -029) were obtained from The Johns Hopkins University. hTERT transformed noncancerous human oral keratinocyte cell line (OKF-6) was a generous gift from James Rheinwald (Harvard University). The DsRed-expressing JHU-013 cell line was established in our laboratory. Human prostate cancer cell line BPH1^{catd} was a generous gift from Simon Hayward (Vanderbilt University). The Huh-7 (liver), SK-HEP-1 (liver), CW2 (colon), Colo-320 (colon), HL-60 (leukemia) and MDA-MB-435s (breast) human cancer cell lines were obtained from the Chinese Academy of Science Shanghai Cell Center (Shanghai, China). The HNSCC, BPH1^{catd}, Colo-320 and CW2 cells were grown in RPMI 1640 medium; the Huh-7 and SK-HEP-1 cells in EMEM; HL-60 cells in IMDM and MDA-MB-435s in L-15 medium. The cultures were supplemented with 10% fetal bovine serum and an antibiotic-antimycotic mixture (100 IU/mL penicillin and 100 µg/mL streptomycin and 0.025µg/mL amphotericin B, Cellgro, Herndon, VA). OKF6 cells were cultured in serum-free keratinocyte medium (GIBCO/Invitrogen, Carlsbad, CA). All cells were grown in 5% CO₂ at 37°C and subcultured at an initial density of 1 × 10⁵ cells/mL every 3 to 4 days. All experiments were performed with cells in the logarithmic phase of growth.

Purification of Sal-B

Sal-B was first extracted from *S. miltiorrhiza* Bunge powder (5 kg) with 20 L of 70% ethanol in Soxhlet extractor. The condensed supernatant was passed through a D101 macroporous resin (column diameter = 12.0 cm, diameter: height = 1:10) and magnesium salt of Sal-B was eluted with a 6-fold column volume of 20–40% ethanol solutions. The Sal-B magnesium salt-rich fraction in 40% ethanol was concentrated under reduced pressure and then adjusted to pH 3–4 with hydrochloric acid for converting the magnesium salt of Sal-B into free Sal-B. The free Sal-B was extracted with ethyl acetate and evaporated at reduced pressure in a low-temperature drying machine. The resultant dry powder was dissolved in 1 L water and applied onto a polyamide chromatographic column (column diameter = 7.0 cm, diameter: height = 1:10). The column was eluted with 10% ethanol, 30% ethanol and then 50% ethanol. The highly purified Sal-B (>95%) eluted in the 50% ethanol solution fraction was then analyzed by high-pressure liquid chromatography (HPLC) with a C-18 column.

3-(4,5-Dimethylthiazol-2-yl)-2,5-diphenyltetrazolium bromide assay

Cells (at a density of 5,000 cells/well) were grown in flat-bottom 96-well cell culture plates in appropriate medium supplemented with 2% fetal bovine serum. The cells were then treated with graded concentrations of Sal-B or celecoxib for 24 hr. Twenty microliters of 3-(4,5-dimethylthiazol-2-yl)-2,5-diphenyltetrazolium bromide (MTT) (5 mg/mL) solution (Sigma, St Louis, MO) were added to each well and then incubated at 37°C for 4 hr. After removing the media, 200 µL of dimethyl sulfoxide were added and left for 30 min at room temperature to dissolve the formazan crystals. The absorbance at 560 nm was measured in a microplate reader (Bio-Rad, Hercules CA).

Colony formation

HNSCC cells were seeded at densities of 300 cells per well in a BD Falcon 6-well tissue culture plate (Palo Alto, CA) and cultured overnight and treated with different concentrations of Sal-B or celecoxib for 24 hr. Following treatment, drug containing medium was replaced with fresh drug-free culture medium (2 mL) and allowed to grow for 7–10 days to permit colony formation from viable clonogenic cells. Colonies formed after ~7 days of continuous culture were stained with 0.1% methylene blue in 50% ethanol. Any colony containing more than 50 cells was considered to represent a viable clonogenic cell.

Hollow fiber assay

The assay was carried out according to the method of Hollingshead *et al.*³⁶ Briefly, 1 × 10⁵ tumor cells were seeded into a 2 cm-long polyvinylidene fluoride hollow fiber with a *M_r* 500,000 cutoff and 1 mm inner diameter (Spectrum Laboratories, Inc., Houston, TX). A maximum of 4 fibers were implanted at both subcutaneous sites (right and left flank) of 6-week-old, female Balb/cA-nu mice (Chinese Academy of Science, Shanghai, China). The mice were given daily intraperitoneal injections of 5-FU or Sal-B for 5 days starting on the third day after fiber implantation. After completion of the treatment, the fibers were removed from the mice and cell viability was analyzed using the MTT assay. Cell growth in each treatment group was compared with growth of untreated control cells. Guidelines for the humane treatment of animals were followed as approved by the TenGen Animal Care and Use Committee.

Human tumor xenografts in athymic nude mice

Four-week-old, Balb/c male athymic nude mice (Nu/Nu) were obtained from Harlan Sprague Dawley, Inc. (Indianapolis, IN). They were provided Harlan Teklad #2018 Global 18% protein rodent diet (Madison, WI) and water *ad libitum*. Mice were housed in temperature-controlled rooms (74 ± 2°F) with a 12-hr alternating light-dark cycle. Three groups (five mice per group) included the Sal-B-treated, celecoxib-treated and untreated groups. Body weights were measured once a week. DsRed expressing JHU-013 cells (2 × 10⁶ cells/100µL/mouse) were injected subcutaneously into the lower backs of the mice using a 25-gauge needle. The mice received Sal-B (80 mg/kg) or celecoxib (5 mg/kg) by intraperitoneal administration every day following JHU-013 cell inoculation. The Sal-B dose for animal treatment was based on the results of the hollow fiber assay and the celecoxib dose was selected on the basis of earlier literature.³⁷ Treatments were continued daily for 24 days. Tumor size was monitored by three-dimensional (3D) *in vivo* magnetic resonance imaging (MRI) and manual measurement with vernier calipers. Guidelines for the humane treatment of animals were followed as approved by the Howard University Animal Care and Use Committee.

In vivo MRI

The *in vivo* monitoring of human tumor xenografts in mice was carried out using a 9.4 T, 89 mm vertical bore NMR spectrometer (Bruker Biospin MRI, Billerica, MA). Before the MRI scan, animals were anesthetized with respiratory administration of 2% isoflurane and gently positioned at the center of the scanner. The total MRI imaging time was less than 1 hr. A 3D imaging technique optimized for T1-weighted image contrast of the tumor and surrounding tissue was implemented in order to accurately track the growth of tumors in mice. The imaging sequence used was a 3D-FLASH with the following parameters: echo time TE = 4–5 msec; repetition time TR = 12–15 msec; flip angle α = 10–15°; field of view 2.56 × 2.56 × 2.0 cm; the matrix size 320 × 320 × 90; voxel size 80 × 80 × 220 µm. For better signal to noise ratio, 4 data acquisitions were used. Tumor volumes were measured by segmenting the tumor and counting the voxels in the region of interest using NIH ImageJ software with a voxel count

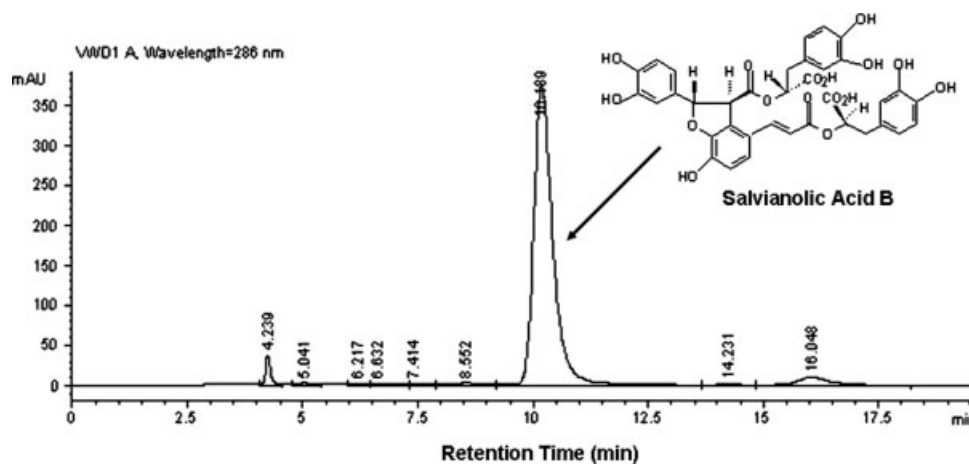


FIGURE 1 – A HPLC profile of Sal-B after passing through the second step of chromatography. The Sal-B peak was located at retention time of 10.2 min through a C-18 column.

plug-in in semiautomatic mode. The tumor volume was calculated by multiplying the total number of voxels by the single voxel volume.

Real-time RT-PCR

RNA was prepared from the treated cells based on the Invitrogen TRIzol protocol (Invitrogen, Carlsbad, CA). First-strand cDNA was synthesized by PCR using a SuperScript III system with oligo(dT) primers (Invitrogen, Carlsbad, CA). The expression levels of COX-1 and COX-2 were measured by taking advantage of real-time RT-PCR using TaqMan[®] Universal PCR Master Mix (Applied Biosystems, Foster City, CA) with COX-1 primer (6-FAM labeled probe, hs00168776_m1) or COX-2 primer (6-FAM labeled probe, Hs00153133_m1). A *beta*-actin (4333762T) primer was used as an endogenous control. The real-time PCR was performed in triplicate for each gene. AmpliTaq Gold Enzyme was first activated at 95°C for 10 min followed by 40 cycles including denaturation at 95°C for 15 sec and annealing at 60°C for 1 min. The data were analyzed using MxPro-Mx3000p software and analyzed using $2^{-\Delta\Delta CT}$ method.⁵⁸

Western immunoblotting

Whole-cell lysates were prepared from treated HNSCC cells incubated with RIPA lysis buffer kit (Santa Cruz Biotechnology, Santa Cruz, CA) and protein concentrations were quantified using a Bio-Rad protein assay (Bio-Rad, Hercules, CA). Whole-cell proteins (30 μ g) were separated by electrophoresis on 8% SDS-polyacrylamide gel and transferred to a polyvinylidene difluoride membrane (Amersham Corp., Arlington Heights, IL). The membrane was then probed sequentially with antibodies against the following proteins: p53, NF- κ B, Bcl-2, Bcl-xL, caspase-3, PARP, COX-2 and β -actin (Sigma, St. Louis, MO). Washed blots were then incubated with horseradish peroxidase conjugated anti-rabbit, anti-mouse or anti-goat antibody (Santa Cruz Biotechnology, Santa Cruz, CA) for 1 hr at room temperature. Blots were developed using a peroxidase reaction and visualized using ECL detection system (Bio-Rad, Hercules, CA).

Flow cytometry

(i) To analyze levels of COX-2 protein, the control and treated cultures of HNSCC cells were treated with PBS-based enzyme-free cell dissociation buffer (Gibco, Carlsbad, CA) to detach cells, which were collected by centrifugation. The collected cells were washed and fixed in chilled 80% ethanol. The fixed cells were washed twice in PBS and then incubated with a solution containing COX-2-FITC (1:200) (Cayman Chemical Company, Ann Arbor, MI) in the dark for 30 min at room temperature. The COX-

2 level was determined using a suitable antibody and a FACStar flow cytometer (Becton Dickinson & Co., San Jose, CA). (ii) To analyze apoptotic cells, the treated HNSCC cells (5×10^4) were collected, washed and fixed as described above. The cells were labeled with annexin V-FITC (Clontech Laboratories, Inc., Palo Alto, CA) and 5 μ g/mL propidium iodide. The expression of annexin V and cell cycle status were analyzed by FACStar flow cytometry. Ten thousand cells per sample were analyzed for both assays.

PGE2 level

PGE2 levels were determined in order to estimate COX-2 activity. JHU-013 cells were treated with or without 100 ng/mL LPS, Sal-B or celecoxib in RPMI 1640 medium with 2% fetal bovine serum for various incubation times. The culture medium was collected and the level of PGE2 was determined by a Correlate-EIA[™] Prostaglandin E₂ Enzyme Immunoassay Kit (Assay Designs, Ann Arbor, MI) and the optical densities were determined by Bio-Rad Microplate Reader (Hercules, CA) at 405 nm. The PGE2 level was calculated as a unit of pg/mL as instructions provided by the manufacture of the assay kit.

Statistical analyses

Results are presented relative to untreated controls. Values represent the mean \pm standard deviation (SD) of a minimum of 3 replicate tests. Data were analyzed by the Duncan test following the ANOVA procedure when multiple comparisons were made. Differences were considered significant when $p < 0.05$.

Results

Preparation of highly purified Sal-B

We first developed a protocol that allowed us to obtain large quantities of highly pure Sal-B from *S. miltiorrhiza* Bge. For this, 5 kg of *S. miltiorrhiza* Bge were subjected to ethanol extraction and Sal-B was first partially purified by macroporous resin chromatography. After acidification, Sal-B was then eluted from a polyamide column. This procedure finally resulted in 136 g of Sal-B of >95% purity. This corresponds to a 2.7% yield, based on total amount of initial raw material (Fig. 1a). Ninety-five percent of pure Sal-B was used in the majority of tests in the present study and partially purified Sal-B fractions of 40%, 60% and 80% purity were also collected to test if impurities antagonized or enhanced the anticancer properties of Sal-B.

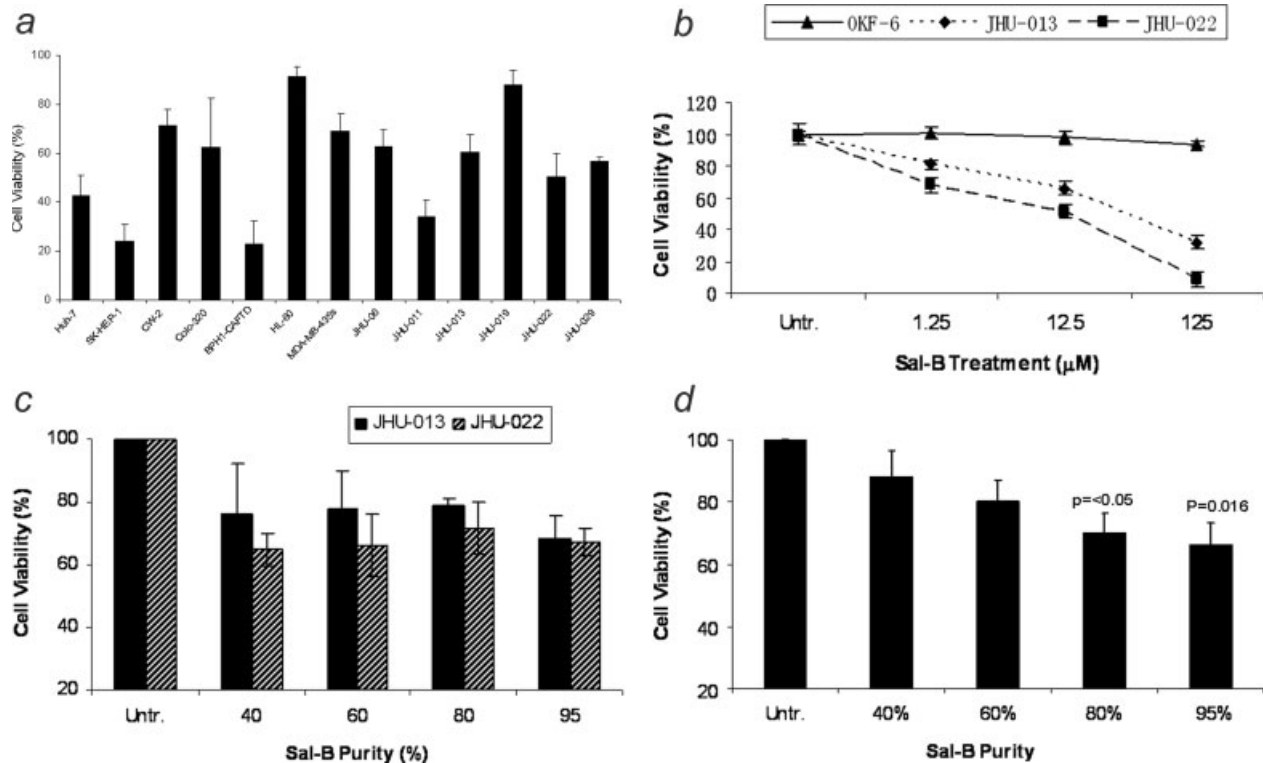


FIGURE 2 – Cytotoxicity of Sal-B on HNSCC cell growth *in vitro*. (a) Thirteen different cell lines were treated with 125 μ M Sal-B for 24 hr and the cell viability was measured by MTT method. The percentage of inhibition on cell viability was compared with parallel untreated cells ($p < 0.05$ in most cell lines excepted in HL-60 and JHU-019 cell lines). (b) OKF-6, JHU-013 and JHU-022 cell lines were treated with Sal-B from 1.25 to 125 μ M for 24 hr and then continued the culture for additional 7 days in Sal-B free condition. The cell viability was measured by colony formation assay. (c) JHU-013 or JHU-022 cells were exposed to same final concentration of Sal-B (125 μ M) using differing stock solutions of Sal-B ranging in purity from 40% to 95% for 24 hr. (d) JHU-013 cells were exposed for 24 hr to the same amount (100 μ g/mL) of powder from Sal-B lots ranging in purity from 40% to 95%. All assays represented the mean \pm SD of 2 independent experiments with triplicate dishes.

Sal-B-inhibits cell viability in several human cancer cell lines tested

A panel of 13 human cancer cell lines, including 6 HNSCC cell lines (JHU-06, -011, -013, -019, -022 and -029), were used in the present study to confirm the cytotoxic effect of Sal-B. All 13 cell lines exhibited decreased cell viability when exposed to 125 μ M Sal-B for 24 hr (Fig. 2a). Compared with the untreated cancer cell lines, the inhibition of cell growth by treatment with Sal-B was statistically significant ($p < 0.05$) in all cell lines except HL-60 and JHU-019 cell lines. The inhibition of cell viability was more pronounced in BPH1^{CAFTD} human prostate tumor cells (76.8%) and SK-HEP-1 human liver cancer cells (75.9%) while HL-60 cells were the least sensitive (8.7%). A 24-hr treatment with Sal-B (125 μ M) caused 40% reduction of cell viability in the majority of HNSCC cell lines (JHU-06, -011, -013, -022 and -029), except JHU-019. Colony formation assays further confirmed the cytotoxicity of Sal-B toward JHU-013, JHU-022 and OKF-6 cell lines (Fig. 2b). Over 30% inhibition occurred with a low-dose of Sal-B treatment (1.25 μ M) in JHU-022 cells and ~20% inhibition in JHU-013 cells. Sal-B treatment caused a dose-dependent decrease in clonogenic potential of the HNSCC cells. Based on colony formation assays, the IC₅₀ values of Sal-B were ~18 μ M in JHU-022 cells and 50 μ M in JHU-013 cells (Fig. 2b). However, there was no cytotoxic effect of Sal-B on the hTERT transformed noncancerous human oral keratinocyte cell line (OKF-6) (Fig. 2b).

There was no significant difference in cytotoxicity when JHU-013 and JHU-022 cell lines were exposed to the same concentration (125 μ M based on Sal-B content) of Sal-B preparations of different levels of purity (Fig. 2c). By contrast, when JHU-013 cells

were exposed to the same amount (100 μ g/mL) of Sal-B fractions differing purity over the 40% to 95% range, cytotoxicity increased in parallel with purity of Sal-B fraction (Fig. 2d). These results show that the impurities in the preparations did not antagonize or potentiate the effect of Sal-B.

Sal-B inhibits growth of JHU-013 cells grown as solid tumor xenografts in vivo

In view of the *in vitro* observations, the effect of Sal-B was further evaluated using Ds-Red expressing JHU-013 cells grown as solid tumor xenografts in immunodeficient mice. To determine a proper dosage for treatment of xenografts in mice, the National Cancer Institute recommended hollow fiber method to determine the potency of Sal-B. The hollow fiber method is recommended for screening natural therapeutic compounds.³⁶ JHU-013 cell were preseeded in the hollow fibers and then transplanted subcutaneously into the flanks of nude mice. Cell viability was determined after the mice completed a short-treatment. Three days after implantation of hollow fibers with cells, the mice were treated daily for 5 days with the clinically used anticancer drug, 5-FU (80 mg/kg/day, 0.1 mL i.p. injection) for 5 days or equal volumes of physiological saline (Fig. 3a). The hollow fibers were recovered and the cell proliferation was estimated using the MTT assay. Treatment with 5-FU caused 35% inhibition of growth when compared with controls treated with physiological saline. Daily treatment with Sal-B for 5 days starting from day 3 after hollow fiber implantation resulted in a dose-dependent inhibition of cell growth with a significant reduction of 41% at a daily dose of 80 mg/kg/day. There was no significant difference between Sal-B and 5-FU at the 80 mg/kg/day dose on the inhibition of JHU-013 cell growth.

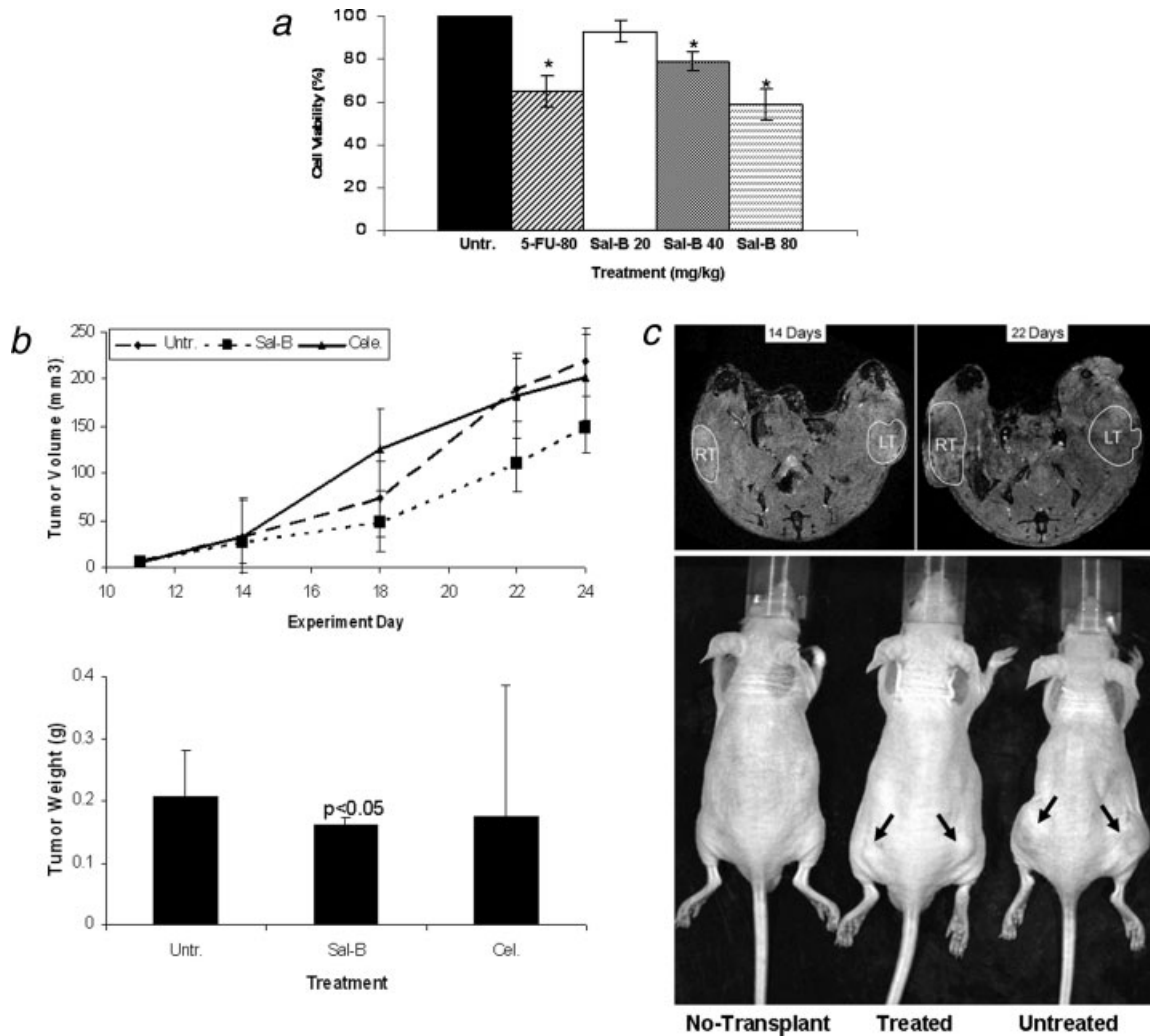


FIGURE 3 – Cytotoxicity of Sal-B on HNSCC cell growth *in vivo*. (a) Hollow fiber assay. The mice were treated with 5-FU (80 mg/kg/day) or different amounts of Sal-B (20 mg, 40 mg, 80 mg/kg/day) by intraperitoneal injection starting on the third day after fiber implantation and the treatments were continued daily for 4 days. The fibers with cells were taken out from the subcutaneous site of mice after a 5-day treatment period and cell viability was measured by MTT method. The levels of cell viability in treated groups were compared with untreated control group (* $p < 0.05$). (b) JHU-013 xenograft growth. The day of DS-Red JHU-013 cells inoculation was the experiment starting day. The mice received Sal-B (80 mg/kg) or celecoxib (5 mg/kg) by intraperitoneal administration every day following JHU-013 cell injection and all mice were sacrificed on day-25. The top panel shows the tumor growth, which was monitored periodically at different days during the 25-day experimental period. The bottom panel shows tumor mass (g) that was measured on the final experiment day immediately after the tumor tissue was removed from the mouse by surgical excision. The average tumor mass is indicated as a bold bar in each group. The p value was compared with untreated group. (c) The right top panel shows the MR images that were taken from the same mouse on experiment day-14 and day-22. The circle indicated the tumor site, right side tumor (RT) and left tumor (LT). The right bottom shows the whole animal image with or without tumor indicated by arrows.

Thus, the hollow fiber tests provided quick and *quasi in vivo* information on Sal-B cytotoxicity toward HNSCC growth and an 80 mg/kg daily treatment dose was selected for the JHU-013 xenograft experiments.

A day after JHU-013 cells were transplanted into the nude mice, daily treatment was initiated with single treatment either with dose Sal-B (80 mg/kg) or celecoxib (5 mg/kg) for 24 days. Each mouse was monitored for tumor growth at least 5 times over the duration of the experiment. Measurement of tumor volume indicated that the Sal-B treatment significantly slowed tumor growth in comparison with the untreated groups (Figs. 3b and 3c). The average tumor weight in the Sal-B group (0.16 g) was also significantly less than in the untreated control group (0.21 g). The average tumor weight in the celecoxib treated groups (0.17 g) is less than untreated group, but a large variation of the tumor weight

was observed in the celecoxib-treated group, ranging from 0.42 g to 0.06 g (Fig. 3b).

Our original plan was to use DsRed-expressing JHU-013 xenografts and monitor with a noninvasive Xenogen IVIS 200 optical imaging system (Xenogen, Hopkinton, MA) to evaluate the treatment effects. However, the optical imaging system failed to clearly detect the DsRed-expressing JHU-013 xenografts because of interference from strong background fluorescence from the skin of the animals. Detection of tumor cell fluorescence was feasible if the tumor was surgically removed and directly exposed under the imaging system. The DsRed fluorescent signal was only found in the tumors and not in spleen, liver, lungs or hearts removed surgically at necropsy. As such, these data indicate that no tumor metastasis developed during the 24 day experiment.

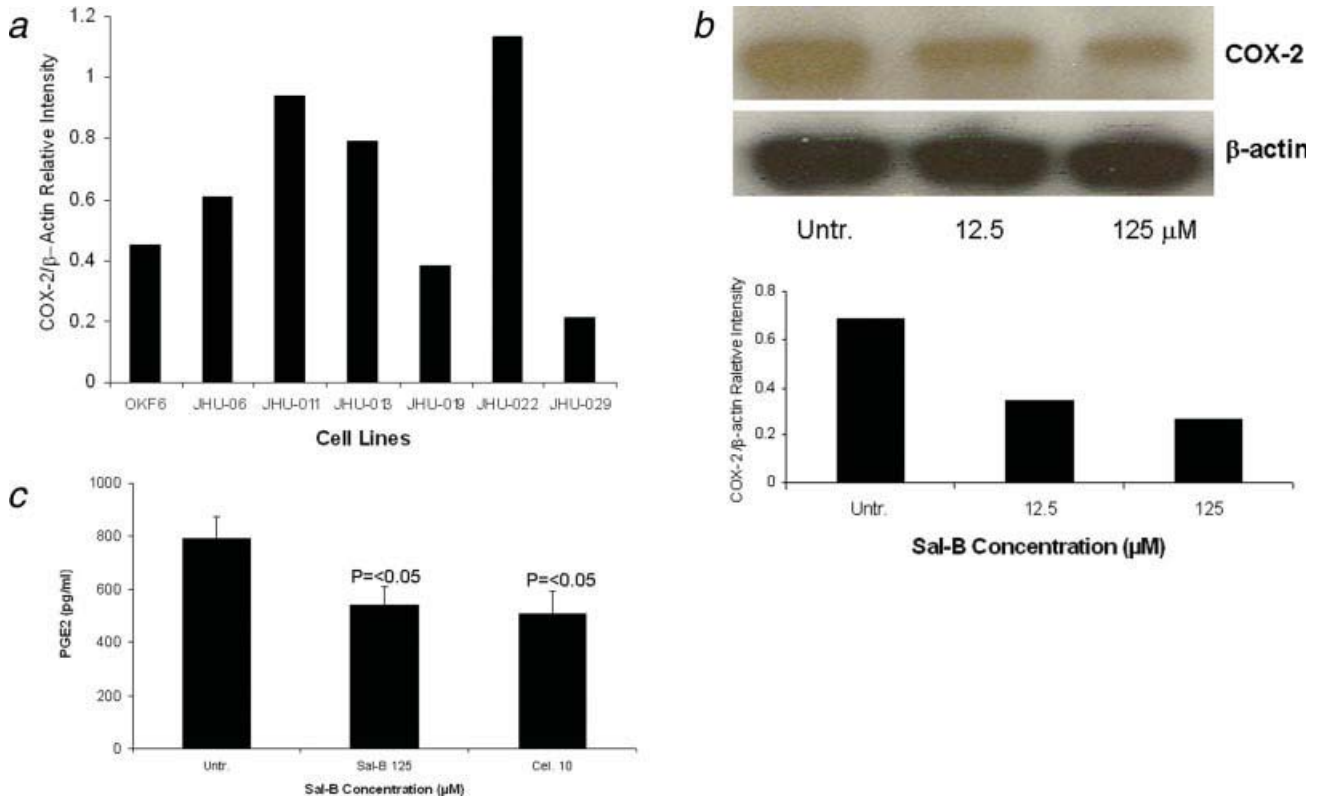


FIGURE 4 – Effect of Sal-B on suppression of PGE2 synthesis. In (a) and (b), the protein levels of COX-2 protein were analyzed by Western blot and semi-quantified based on COX-2/β actin related intensity. (a) COX-2 protein levels in 6 HNSCC cell lines and a noncancerous human oral keratinocyte cell line (OKF-6). (b) COX-2 protein levels from JHU-013 cells treated with Sal-B (12.5 and 125 μM) for 24 hr. (c) The PGE2 levels were measured after JHU-013 cells treated with Sal-B (125 μM) or celecoxib (10 μM) for 24 hr. The PGE2 levels are expressed as pg/mL of total cell culture. The results represented the mean ± SD of 2 independent experiments with triplicate dishes. The *p* value was compared with untreated group. [Color figure can be viewed in the online issue, which is available at www.interscience.wiley.com.]

Inhibition of COX-2 expression by Sal-B

The effects were analyzed using Western blot (Figs. 4a and 4b), enzymatic assay (Fig. 4c), flow cytometry (Fig. 5a) and real-time RT-PCR (Fig. 5b) in 6 different JHU HNSCC cell lines grown *in vitro* or *in vivo*. To determine whether Sal-B is capable of inhibiting COX-2 overexpression in HNSCC, we first carefully reviewed the COX-2 protein levels in all 6 HNSCC cell lines, as compared with a transformed noncancerous human oral keratinocyte cell line (OKF-6) (Fig. 4a). The levels of COX-2 protein were higher in JHU-06, -011, -013 and -022 cell lines compared with the levels in OKF6, but were not in JHU-019 and -029 cell lines. Interestingly, COX-2 protein levels in JHU-022 cells were significantly decreased by 50–61% following 24-hr treatment with different concentrations of Sal-B ranging from 12.5 μM and 125 μM (Fig. 4b). Treatment of JHU-013 cells with Sal-B (125 μM) and celecoxib (10 μM) decreased PGE2 levels by 32% and 36% when compared with drug-free control cultures (Fig. 4c). Flow cytometry analysis (Fig. 5a) showed that COX-2 protein levels were noticeably reduced in JHU-013 cells treated *in vitro* with Sal-B or celecoxib. COX-2 protein levels were also lower in cells obtained by disaggregation of JHU-013 solid tumor xenografts removed surgically from the treated mice. The COX-2 protein levels were significantly lower in the Sal-B and celecoxib treated groups in the isolated cells (Fig. 5a).

Sal-B selectively inhibits COX-2 expression in JHU-013 cells

To determine whether Sal-B can selectively inhibit COX-2, we used real-time RT-PCR with specific COX-1 or COX-2 primers (Fig. 5b) and confirmed the results in LPS stimulated cells (Figs. 5c and 5d). There was no statistically significant change in the

mRNA levels of COX-1 after JHU-013 cells were treated with gradually increasing doses of Sal-B. The mRNA levels of COX-2, however, were reduced at least 18-fold compared with COX-1 when JHU-013 cells were exposed to 250 μM Sal-B for 24 hr. In addition, a dose-dependent decrease in COX-2 mRNA level was observed when JHU-013 cells were exposed to graded doses of Sal-B from 12.5 to 250 μM.

We confirmed the selective inhibitory effect of Sal-B on LPS stimulation of COX-2 activity in the JHU-013 cell system. The level of COX-2 activity increased in a time-dependent manner with increasing the exposure time of JHU-013 cells to 100 ng/mL LPS (Fig. 5c). PGE2 level increased ~4-fold when JHU-013 cells were exposed to LPS (100 ng/mL) for 4 hr, compared with untreated JHU-013 cells (Fig. 5c). In contrast, a dose-dependent inhibition was observed when JHU-013 cells were exposed to LPS and Sal-B (12.5 μM to 250 μM) and the PGE2 level was reduced by more than 88% when the LPS stimulated JHU-013 cells were exposed to 125 μM Sal-B (Fig. 5c). A similar inhibitory pattern was revealed by flow cytometry studies using FITC-conjugated anti-COX-2 antibody for detection of the protein in JHU-013 cells treated with LPS and Sal-B (Fig. 5d). The levels of COX-2 protein decreased in a dose-dependent manner on treatment with Sal-B when compared with LPS-stimulated control cells.

Effects of Sal-B on apoptosis

To better understand the cytotoxic effects in HNSCC growth, we further investigated the effect of Sal-B on apoptosis. We found that Sal-B induced caspase-dependent apoptosis in JHU-013 cells. The numbers of apoptotic cells gradually increased when increasing exposure time with 125 μM Sal-B (Figs. 6a and 6b). In con-

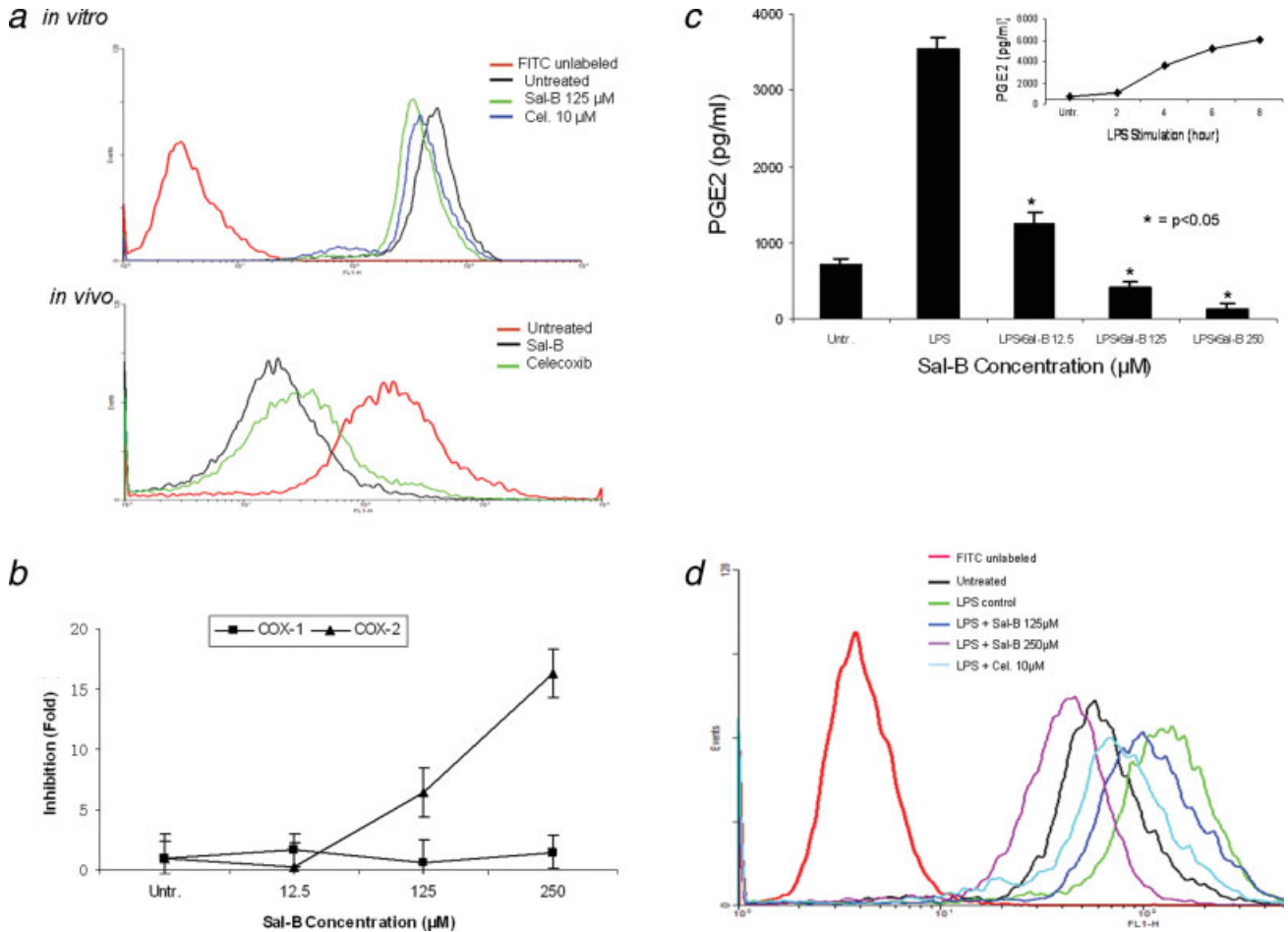


FIGURE 5 – Sal-B selectively inhibits COX-2 expression. (a) COX-2 protein levels were analyzed by flow cytometry with FITC-conjugated COX-2 antibody after treatment of JHU-013 cells with Sal-B or celecoxib. The top panel shows COX-2 levels in cultured JHU-013 cells treated with 125 μ M Sal-B or 10 μ M celecoxib for 24 hr. The bottom panel shows the COX-2 levels of JHU-013 cells isolated by disaggregation of tumors with the different treatment groups. (b) The inhibitory rate on the mRNA levels of COX-1 and COX-2 were analyzed by real-time PCR with specific COX-1 or COX-2 primers after JHU-013 cells treated with graded concentrations of Sal-B (12.5, 125 and 250 μ M) for 24 hr. (c) An enzyme immunoassay was used to determine the levels of PGE2 in JHU-013 cells were exposed for 4 hr to LPS (100 ng/mL) with or without Sal-B (12.5, 125 or 250 μ M). Insert on the top-right is the PGE2 level measured after treatment of JHU-013 cells with LPS (100 ng/mL) alone for 2 to 8 hr. The PGE2 levels are reported in terms of pg/mL. The results from PGE2 analysis represent the mean \pm SD of 2 independent experiments with triplicate dishes. The p value was compared with LPS treated alone ($*p < 0.05$). (d) The JHU-022 cells were exposed to LPS (100 ng/mL) with or without Sal-B from 12.5 to 250 μ M for 4 hr, and then the COX-2 levels were analyzed by flow cytometry with FITC-conjugated COX-2 antibody.

tract, over 70% JHU-013 cells were undergone apoptosis when the cells exposed to 250 μ M Sal-B for 3 hr (Figs. 6a and 6b). The expression levels of caspase 3 and associated cleavage of PARP were also evaluated by western blot analysis (Fig. 6b). The level of caspase 3 was significantly increased after JHU-013 cells exposed to 125 μ M Sal-B for 24 hr. Moreover, Sal-B also caused PARP cleavage as revealed by the generation of an 85-kDa fragment following the 24-hr treatment. This is evidence for caspase-dependent apoptosis in Sal-B treated JHU-013 cells. In addition, Sal-B also regulated the expression of proteins associated with apoptosis, such as NF- κ B, p53, MDM-2, Bcl-2 and Bcl-xL (Fig. 6c). The levels of NF- κ B, MDM-2, Bcl2 and Bcl-xL were clearly lower after cells were exposed to 125 μ M Sal-B for 6 hr. The level of p53 was in cells exposed to Sal-B for 24 hr (Fig. 6c).

Discussion

As documented by the World Health Organization, at least one-third of all cancer cases are preventable and prevention offers the most cost-effective long-term strategy. Indeed, about 20% of all

human cancers are caused by chronic infection or chronic inflammatory states.³⁹ Therefore, controlling chronic inflammation is an attractive strategy for cancer prevention. Prostaglandins produced by the action of COX-2 on arachidonic acid are involved in chronic inflammation. There is accruing evidence to suggest that chronic inflammation sets the stage for changes leading to cancer development. This provides the scientific rationale for the use of celecoxib, a NSAID selective COX-2 inhibitor, in cancer prevention. Hence, celecoxib received accelerated approval from the FDA for treatment of adenomas in high-risk familial adenomatous polyposis patients.^{40,41} However, celecoxib-related cardiovascular risk is reported to increase from 2.3% to 3.4% when patients receive 200 mg to 400 mg of celecoxib twice daily.²² The safety of celecoxib is indeed a major concern in cancer chemoprevention and the increased risk of cardiovascular events limits long-term use of celecoxib for chemoprevention.

In this study, we report that Sal-B, which is isolated from a Chinese herbal medicine *S. multiorrhiza* Bge, inhibits the growth of human head and neck squamous cell carcinoma cells both *in vitro* and *in vivo* through inhibition of COX-2 expression and induction

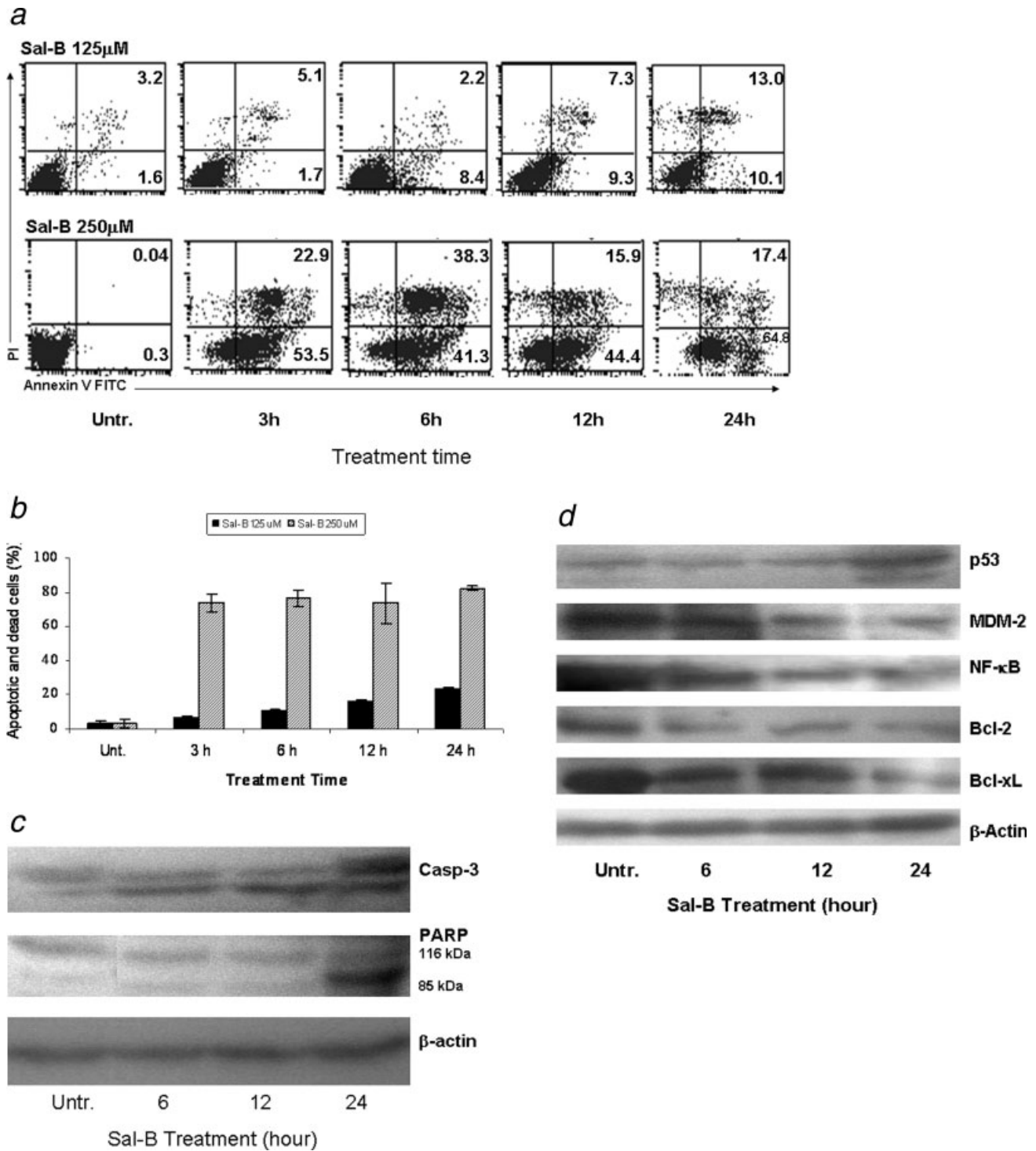


FIGURE 6 – Effect of Sal-B on induction of apoptosis in JHU-013 cells. JHU-013 cells were cultured with either Sal-B 125 μ M or 250 μ M for 3, 6, 12 and 24 hr followed by measurement of Annexin V protein in the cell membrane by flow cytometry using FITC-conjugated Annexin V antibody. The cells were also stained with propidium iodide (PI). (a) The scatter display of flow cytometry analysis: the bottom right quadrant of each panel displays V-FITC-positive and PI-negative cells indicating that the cells were in an early stage of apoptosis and cells in the top right quadrant stained with both PI and Annexin V, indicating that the cells were in late apoptosis or no longer viable. (b) Histogram of flow cytometry analysis: the levels of apoptotic and dead cells from Sal-B treated JHU-013 cells (125 μ M, solid bars; 250 μ M, shaded bars). The data was shown as mean \pm SD ($p < 0.05$). (c) and (d) JHU-013 cells exposed to Sal-B (125 μ M) for 6, 12 and 24 hr, expression levels of apoptotic markers were evaluated by Western blot with antibody probes for apoptosis regulatory proteins, such as caspase-3, p53, MDM-2, NF- κ B, Bcl-2 and Bcl-xL. The levels of PARP expression and degradation were also analyzed by Western blot to estimate the levels of intact PARP (116 kD) and its cleaved form (85 kD). The amount of protein was normalized by comparing the intensity of the β -actin band.

of apoptosis. We investigated the cytotoxic effects of Sal-B *in vitro* using the MTT method to provide a quick assessment of drug response. The IC₅₀ values of Sal-B for inhibition of HNSCC JHU-013 and JHU-022 cell growth were determined using a more sensitive and reliable colony formation method.⁴² This effect of Sal-B was further supported by experiments using the hollow fiber method and the tumor xenografts. The results confirmed that Sal-B greatly suppressed HNSCC tumor growth compared with untreated and treatment with celecoxib.

Both COX-1 and COX-2 can convert arachidonic acid to prostaglandins, which are involved in pain, inflammation, cell proliferation and other biologic responses. Unlike COX-1, which is normally present in most tissues of the human body as a housekeeping enzyme, COX-2 is induced by inflammation. Usually COX-2 expression in normal tissues is low compared that in tumors. The levels of COX-2 can increase even in normal tissues and in stromal cells when challenged by immunogenic or inflammatory stimulus. In addition, while COX-1 and COX-2 share some common biologic functions, they are part of diverse cell-signaling pathways. Numerous studies have indicated that overexpression of COX-2 occurs in many cancers including HNSCC. Our data clearly demonstrate that Sal-B as a single agent is capable of selectively suppressing COX-2 expression in the presence or absence of LPS stimulation. Interestingly, we found that this effect of Sal-B is more sensitive under conditions of high COX-2 expression. For example, a dose of 125 μ M Sal-B sharply reduced PGE2 levels by more than 80% in LPS-stimulated JHU-013 cells (Fig. 5c) but only caused a 32% reduction in PGE-2 levels in the unstimulated condition (Fig. 4c). JHU-011 and JHU-022 cell lines are more sensitive to the growth inhibitory effects of Sal-B than JHU-019 cell line. Interestingly, JHU-011 and JHU-022 have high levels of COX-2 expression, whereas JHU-019 has low-level of COX-2 expression (Figs. 2a and 4a).

Overexpression of COX-2 in tumor cells has been shown to increase the proto-oncogene Bcl-2 and lead to inhibition of apoptosis.⁴³ The effect of COX-2 derived from stromal cells on proto-oncogene expression in tumors is a matter of conjecture. It is reasonable to assume that Sal-B and celecoxib would inhibit COX-2

expression in tumors and associated stroma. Sal-B induces caspase-dependent apoptosis in JHU 013 cells as shown by cleavage of a caspase substrate, poly (ADP) ribose polymerase (PARP). Sal-B also decreased the cellular amounts of antiapoptotic proteins such as NF- κ B, MDM-2, Bcl-2 and Bcl-xL and increased proapoptotic proteins such as p53 and caspase 3. Taken together, these data suggest that the anticancer effects of Sal-B are through a COX-2-dependent pathway to inhibit PGE2-synthesis as well as a COX-2-independent pathway to regulate apoptosis of HNSCC.

S. Miltiorrhiza, as a traditional Chinese medicine has been safely used in treating neoplastic diseases and chronic inflammation in oriental countries based on long history of clinical evidence. *S. miltiorrhiza* bge usually contains 1–7% Sal-B depending on geographical source and harvest season. Based on the People's Republic of China Pharmacopoeia (2005 edition).⁴⁴ When *S. miltiorrhiza* bge is sold as an herbal medicine, it must contain at least 3% Sal-B by weight of the raw material. Commercially available Danshen capsule is formulated from the extract of *S. miltiorrhiza* bge that contains a minimum of 11 mg Sal-B according to the People's Republic of China Pharmacopoeia (2005 edition). A daily dose of 9–12 capsules (3 or 4 capsules taken 3 times a day) has been recommended as a dietary supplement for prevention of cardiovascular diseases in China. In mice, the LD₅₀ value of *S. miltiorrhiza* bge is \sim 27 g/kg/day.⁴⁵ A long-term toxicity study of *S. miltiorrhiza* bge reported that 18% of rats (4/22) showed some reversible hepatomegaly when they received *S. miltiorrhiza* glucose (5 g *S. miltiorrhiza* bge/kg/day) *via* intraperitoneal route. The hepatomegaly was resolved on discontinuation of *S. miltiorrhiza* glucose.⁴⁶ Therefore, the experimental dose of Sal-B (80 mg/kg/day) is in a safe range for the animal, but more toxicity tests are needed for extrapolation to the clinical setting for humans. This study demonstrates the potential of Sal-B as an effective and safe natural anticancer agent for HNSCC prevention and treatment.

Acknowledgements

The authors thank Ms. Dan Zhang, Mr. Songping Wang, and Ms. Ailin Zhu for their excellent technical assistance in the animal experiments and thank Dr. Carmen Sato-Bigbee for valuable discussion.

References

- Parkin DM, Bray F, Ferlay J, Pisani P. Global cancer statistics, 2002. *CA Cancer J Clin* 2005;55:74–108.
- Jemal A, Siegel R, Ward E, Hao Y, Xu J, Murray T, Thun MJ. Cancer statistics, 2007. *CA Cancer J Clin* 2007;57:43–66.
- Lippman SM, Sudbo J, Hong WK. Oral cancer prevention and the evolution of molecular-targeted drug development. *J Clin Oncol* 2005;23:346–56.
- Forastiere A, Koch W, Trotti A, Sidransky D. Head and neck cancer. *N Engl J Med* 2001;345:1890–900.
- Gourin C, Podolsky R. Racial disparities in patients with head and neck squamous cell carcinoma. *Laryngoscope* 2006;116:1093–106.
- Lin DT, Subbaramaiah K, Shah J, Dannenberg AJ, Boyle JO. Cyclooxygenase-2: a novel molecular target for the prevention and treatment of head and neck cancer. *Head Neck* 2002;24:792–9.
- Kelloff G, Lippman SM, Dannenberg AJ, Sigman CC, Pearce HL, Reid BJ, Szabo E, Jordan VC, Spitz MR, Mills GB, Papadimitrakopoulou VA, Lotan R, et al. AACR Task Force on Cancer Prevention. Progress in chemoprevention drug development: the promise of molecular biomarkers for prevention of intraepithelial neoplasia and cancer—a plan to move forward. *Clin Cancer Res* 2006;12:3661–97.
- Gu X, Song X, Dong Y, Cai H, Walters E, Zhang R, Pang X, Xie T, Guo Y, Sridhar R, Califano JA. Vitamin E succinate induces ceramide-mediated apoptosis in human head and neck squamous cell carcinoma *in vitro* and *in vivo*. *Clin Cancer Res* 2008;14:1840–8.
- Wang Z. The role of COX-2 in oral cancer development, and chemoprevention/treatment of oral cancer by selective COX-2 inhibitors. *Curr Pharm Des* 2005;11:1771–7.
- Moraitis D, Du B, De Lorenzo MS, Boyle JO, Weksler BB, Cohen EG, Carew JF, Altorki NK, Kopelovich L, Subbaramaiah K, Dannenberg AJ. Levels of cyclooxygenase-2 are increased in the oral mucosa of smokers: evidence for the role of epidermal growth factor receptor and its ligands. *Cancer Res* 2005;65:664–70.
- Li N, Sood S, Wang S, Fang M, Wang P, Sun Z, Yang CS, Chen X. Overexpression of 5-lipoxygenase and cyclooxygenase 2 in hamster and human oral cancer and chemopreventive effects of zileuton and celecoxib. *Clin Cancer Res* 2005;11:2089–96.
- Bergmann C, Strauss L, Zeidler R, Lang S, Whiteside TL. Expansion of human T regulatory type 1 cells in the microenvironment of cyclooxygenase 2 overexpressing head and neck squamous cell carcinoma. *Cancer Res* 2007;67:8865–73.
- Chang HW, Roh JL, Jeong EJ, Lee SW, Kim SW, Choi SH, Park SK, Kim SY. Wnt signaling controls radiosensitivity via cyclooxygenase-2-mediated Ku expression in head and neck cancer. *Int J Cancer* 2008;122:100–7.
- Gross ND, Boyle JO, Morrow JD, Williams MK, Moskowitz CS, Subbaramaiah K, Dannenberg AJ, Duffield-Lillico AJ. Levels of prostaglandin E metabolite, the major urinary metabolite of prostaglandin E₂, are increased in smokers. *Clin Cancer Res* 2005;11:6087–93.
- Schunor R, Brieger J, Franke RL, Jakob R, Mann WJ. Increased PGE2 levels in nonmalignant mucosa adjacent to squamous cell carcinoma of the head and neck. *ORL J Otorhinolaryngol Relat Spec* 2005;67:96–100.
- Chang MC, Wu HL, Lee JJ, Lee PH, Chang HH, Hahn LJ, Lin BR, Chen YJ, Jeng JH. The induction of prostaglandin E₂ production, interleukin-6 production, cell cycle arrest, and cytotoxicity in primary oral keratinocytes and KB cancer cells by areca nut ingredients is differentially regulated by MEK/ERK activation. *J Biol Chem* 2004;279:50676–83.
- Zhang DY, Wu J, Ye F, Xue L, Jiang S, Yi J, Zhang W, Wei H, Sung M, Wang W, Li X. Inhibition of cancer cell proliferation and prostaglandin E₂ synthesis by *Scutellaria baicalensis*. *Cancer Res* 2003;63:4037–43.
- Bertagnolli MM, Eagle CJ, Zauber AG, Redston M, Solomon SD, Kim K, Tang J, Rosenstein RB, Wittes J, Corle D, Hess TM, Woloj GM, et al. APC Study Investigators. Celecoxib for the prevention of sporadic colorectal adenomas. *N Engl J Med* 2006;355:873–84.

19. Arber N, Eagle CJ, Spicak J, Rác I, Dite P, Hajer J, Zavoral M, Lechuga MJ, Gerletti P, Tang J, Rosenstein RB, Macdonald K, et al; PreSAP Trial Investigators. Celecoxib for the prevention of colorectal adenomatous polyps. *N Engl J Med* 2006;355:885–95.
20. Nelson N. Years of research come to fruition with launch of oral cancer prevention trial. *J Nat Cancer Inst* 2006;98:88–9.
21. Patel MI, Subbaramaiah K, Du B, Chang M, Yang P, Newman RA, Cordon-Cardo C, Thaler HT, Dannenberg AJ. Celecoxib inhibits prostate cancer growth: evidence of a cyclooxygenase-2-independent mechanism. *Clin Cancer Res* 2005;11:1999–2007.
22. Solomon SD, McMurray J, Pfeffer M, Wittes J, Fowler R, Finn P, Anderson WF, Zauber A, Hawk E, Bertagnolli M; Adenoma Prevention with Celecoxib (APC) Study Investigators. Cardiovascular risk associated with celecoxib in a clinical trial for colorectal adenoma prevention. *N Engl J Med* 2005;352:1071–80.
23. Walters R. Chinese medicine and cancer, vol. 239. 2006:281–91. (Excerpted with permission from Walters R. *Options: The Alternative Cancer Therapy Book*, Garden City Park, New York: Avery Publishing Inc., 1993).
24. Wu J. *An illustrated Chinese Materia Medica*. Oxford University Press, 2005. 706.
25. Wang X, Morris-Natschke SL, Lee KH. New developments in the chemistry and biology of the bioactive constituents of Tanshen. *Med Res Rev* 2007;27:133–48.
26. Huang KC, ed. *The pharmacology of Chinese herbs*. CRC publishers, 1992. 388.
27. National Pharmacopoeia Council of China. *Chinese Pharmacopoeia, Part I*, 2005 edition. Beijing: Chemical Industry Publishing Company, 2005. 52 p.
28. Hu P, Luo GA, Zhao Z, Jiang ZH. Quality assessment of radix *Salviae miltiorrhizae*. *Chem Pharm Bull* 2005;53:481–6.
29. Zhu H, Xie T, Gu X, Ji H, Yang Y, Ge M, Song X, Xue J. Antitumor effect of salvianolic acid B. *Chin J Practical Med* 2004;4:2224–6.
30. Zhou ZT, Yang Y, Ge JP. The preventive effect of salvianolic acid B on malignant transformation of DMBA-induced oral premalignant lesion in hamsters. *Carcinogenesis* 2006;27:826–32.
31. Efferth T, Kahl S, Paulus K, Adams M, Rauh R, Boeczelt H, Hao X, Kaina B, Bauer R. Phytochemistry and pharmacogenomics of natural products derived from traditional Chinese medicine and Chinese materia medica with activity against tumor cells. *Mol Cancer Ther* 2008;7:152–61.
32. Chen YH, Lin SJ, Chen YL, Liu PL, Chen JW. Anti-inflammatory effects of different drugs/agents with antioxidant property on endothelial expression of adhesion molecules. *Cardiovasc Hematol Disord Drug Targets* 2006;6:279–304.
33. Liu CS, Cheng Y, Hu JF, Zhang W, Chen NH, Zhang JT. Comparison of antioxidant activities between salvianolic acid B and Ginkgo biloba extract (EGb 761). *Acta Pharmacol Sin* 2006;27:1137–45.
34. Zhu YZ, Huang SH, Tan BK, Sun J, Whiteman M, Zhu YC. Antioxidants in Chinese herbal medicines: a biochemical perspective. *Nat Prod Rep* 2004;21:478–89.
35. Chen YL, Hu CS, Lin FY, Chen YH, Sheu LM, Ku HH, Shiao MS, Chen JW, Lin SJ. Salvianolic acid B attenuates cyclooxygenase-2 expression in vitro in LPS-treated human aortic smooth muscle cells and in vivo in the apolipoprotein-E-deficient mouse aorta. *J Cell Biochem* 2006;98:618–31.
36. Hollingshead MG, Alley MC, Camalier RF, Abbott BJ, Mayo JG, Malspeis L, Grever MR. In vivo cultivation of tumor cells in hollow fibers. *Life Sci*. 1995;57:131–41.
37. Adhami VM, Malik A, Zaman N, Sarfaraz S, Siddiqui IA, Syed DN, Afaq F, Pasha FS, Saleem M, Mukhtar H. Combined inhibitory effects of green tea polyphenols and selective cyclooxygenase-2 inhibitors on the growth of human prostate cancer cells both in vitro and in vivo. *Clin Cancer Res* 2007;13:1611–9.
38. Livak KJ, Schmittgen TD. Analysis of relative gene expression data using real-time quantitative PCR and the $2^{-\Delta\Delta C_T}$ method. *Methods* 2001;25:402–8.
39. De Marzo AM, Platz EA, Sutcliffe S, Xu J, Grönberg H, Drake CG, Nakai Y, Isaacs WB, Nelson WG. Inflammation in prostate carcinogenesis. *Nat Rev Cancer* 2007;7:256–69.
40. Kelloff G, Sigman C. Assessing intraepithelial neoplasia and drug safety in cancer-preventive drug development. *Nat Rev Cancer* 2007;7:508–18.
41. Steinbach G, Lynch P, Phillips RK, Wallace MH, Hawk E, Gordon GB, Wakabayashi N, Saunders B, Shen Y, Fujimura T, Su LK, Levin B, et al. The effect of celecoxib, a cyclooxygenase-2 inhibitor, in familial adenomatous polyposis. *N Engl J Med* 2000;342:1946–52.
42. Kosaka T, Fukaya K, Tsuboi S, Pu H, Ohno T, Tsuji T, Namba M. Comparison of various methods of assaying the cytotoxic effects of ethanol on human hepatoblastoma cells (HUH-6 line). *Acta Med Okayama* 1996;50:151–6.
43. Tsujii M, DuBois RN. Alterations in cellular adhesion and apoptosis in epithelial cells overexpressing prostaglandin endoperoxide synthase 2. *Cell* 1995;83:493–501.
44. The State Pharmacopoeia Commission of People's Republic of China. *The People's Republic of China Pharmacopoeia, 2005, vol. I*. Beijing: Chemical Industry Press, 2005. 394.
45. Yang J, Gui C, Xiong Y, Chen G, Ding B, Song J. Study on acute and topical toxicity of Danshen glucose injection. *Acta Academiae Mediciae Wannan* 2007;1:11–3.
46. Han J, Liu X, Xu Y, Wang W, Ma Z, Xiong Y. Long-term toxicity study of *Salvia miltiorrhiza* glucose injection in rats. *Acta Academiae Mediciae Wannan* 2005;4:248–52.